

PRECISION MEASUREMENT OF THE ANOMALOUS MAGNETIC MOMENT OF THE MUON

C.S. Özben², G.W. Bennett², B. Bousquet⁹, H.N. Brown², G.M. Bunce², R.M. Carey¹, P. Cushman⁹, G.T. Danby², P.T. Debevec⁷, M. Deile¹¹, H. Deng¹¹, W. Deninger⁷, S.K. Dhawan¹¹, V.P. Druzhinin³, L. Duong⁹, E. Efsthadiadis¹, F.J.M. Farley¹¹, G.V. Fedotovitch³, S. Giron⁹, F.E. Gray⁷, D. Grigoriev³, M. Grosse-Perdekamp¹¹, A. Grossmann⁶, M.F. Hare¹, D.W. Hertzog⁷, X. Huang¹, V.W. Hughes¹¹, M. Iwasaki¹⁰, K. Jungmann⁵, D. Kawall¹¹, B.I. Khazin³, J. Kindem⁹, F. Krienen¹, I. Kronkvist⁹, A. Lam¹, R. Larsen², Y.Y. Lee², I. Logashenko¹, R. McNabb⁹, W. Meng², J. Mi², J.P. Miller¹, W.M. Morse², D. Nikas², C.J.G. Onderwater⁷, Y. Orlov⁴, J.M. Paley¹, Q. Peng¹, C.C. Polly⁷, J. Pretz¹¹, R. Prigl², G. zu Putnitz⁶, T. Qian⁹, S.I. Redin^{3,11}, O. Rind¹, B.L. Roberts¹, N.M. Ryskulov³, P. Shagin⁹, Y.K. Semertzidis², Yu.M. Shatunov³, E.P. Sichtermann¹¹, E. Solodov³, M. Sossong⁷, A. Steinmetz¹¹, L.R. Sulak¹, A. Trofimov¹, D. Urner⁷, P. von Walter⁶, D. Warburton² and A. Yamamoto⁸.

¹*Boston University, Boston, Massachusetts 02215, USA*

²*Brookhaven National Laboratory, Physics Dept., Upton, NY 11973, USA*

³*Budker Institute of Nuclear Physics, Novosibirsk, Russia*

⁴*Newman Laboratory, Cornell University, Ithaca, NY 14853, USA*

⁵*Kernfysich Versneller Instituut, Rijksuniversiteit Groningen, Netherlands*

⁶*University of Heidelberg, Heidelberg 69120, Germany*

⁷*University of Illinois, Physics Dept., Urbana-Champaign, IL 61801, USA*

⁸*KEK, High Energy Acc. Res. Org., Tsukuba, Ibaraki 305-0801, Japan*

⁹*University of Minnesota, Physics Dept., Minneapolis, MN 55455, USA*

¹⁰*Tokyo Institute of Technology, Tokyo, Japan*

¹¹*Yale University, Physics Dept., New Haven, CT 06511, USA*

ABSTRACT

The muon $g-2$ experiment at Brookhaven National Laboratory measures the anomalous magnetic moment of the muon, a_μ , very precisely. This measurement tests the Standard Model. The analysis for the data collected in 2000 (a μ^+ run) is completed and the accuracy on a_μ is improved to 0.7 ppm, including statistical and systematic errors. The data analysis was performed blindly between the precession frequency and the field analysis groups in order to prevent a possible bias in the a_μ result. The result is $a_\mu(\text{exp}) = 11\,659\,204(7)(5) \times 10^{-10}$ (0.7 ppm). This paper features a detailed description of one of the four analyses and an update of the theory.

1 Introduction

The gyromagnetic ratio (g-factor) of a particle is defined as the ratio of its magnetic moment to its spin angular momentum. For a point-like spin-1/2 particle, the g value is predicted by the Dirac equation to be equal to 2. On the other hand, from experiments on the hyperfine structure of hydrogen in the late 1940's, it was found that the g value of an electron was not exactly 2 (≈ 2.002). In the first order this deviation is due to the creation and absorption of a virtual photon by the particle. This process is described by quantum electrodynamics (QED) and the electron g-2 experiments were precise tests of QED. The Standard Model (SM) calculations for the anomalous magnetic moment of the muon includes also the small contributions from hadronic and weak interactions, in addition to electromagnetic (QED) interactions. The QED contribution to the SM is the largest, however it is the most precisely known. On the other hand, the largest contribution to the a_μ uncertainty comes from the hadronic interactions.

2 Experimental Method and Apparatus

When a positive muon decays into a positron and two neutrinos, parity is maximally violated so that the average positron momentum is along the muon spin direction (in the muon rest frame). Since observing the decay energy in the laboratory frame is equivalent to observing the decay angle in the center-of-mass system, the muon spin direction can be measured by counting the decay positrons above a certain energy threshold. As a result, the positron counting rate is modulated with the muon spin precession. This is the main concept of the muon g-2 experiments.¹

In our experiment, polarized muons are injected into a superconducting storage ring. The ring provides a very uniform static dipole magnetic field, \vec{B} . If the g-factor of a muon were exactly equal to two, the spins and the momenta of the muons would stay parallel during the storage. This would mean the cyclotron frequency, ω_c , of the muon is equal to the spin precession frequency, ω_a . However, due to the anomaly on the magnetic moment, the spin precesses faster than the momentum, $\omega_s = \omega_c(1 + a_\mu\gamma)$. The muon spin precession angular frequency relative to its momentum in the presence of a vertical focusing electric field \vec{E} and magnetic field is given by:

$$\vec{\omega}_a = -\frac{e}{mc} \left[a_\mu \vec{B} - \left(a_\mu - \frac{1}{\gamma^2 - 1} \right) \vec{\beta} \times \vec{E} \right] \quad (1)$$

where a_μ is the muon anomalous magnetic moment and γ is the relativistic Lorentz factor.

The influence of the electric field on ω_a is eliminated by using muons with the “magic” momentum $\gamma_\mu = 29.3$, for which $P = 3.09 \text{ GeV}/c$. The measurement of the angular precession frequency ω_a and static field B measured in terms of the proton NMR frequency, ω_p , determines a_μ as follows;

$$a_\mu = \frac{\frac{\omega_a}{\omega_p}}{\lambda - \frac{\omega_a}{\omega_p}} \quad (2)$$

where $\lambda = \mu_\mu/\mu_p = 3.183\,345\,39(10)$.²

The counting rate $N(t)$ of decay positrons with energies above an energy threshold E is modulated by the spin precession of the muon, ideally leading to

$$N(t) = N_0(E) e^{-t/\tau_\mu} (1 + A \cos[\omega_a t + \phi]) \quad (3)$$

where N_0 is the normalization, τ_μ is the time-dilated muon lifetime, A is the energy-dependent asymmetry and ϕ is the phase. The angular precession frequency ω_a is determined from a fit to the experimental data. Figure 1 shows the g-2 precession frequency data collected in 2000. The error bars are in blue. Figure 2 shows the comparison of the energy spectrum at the peak and the trough of the g-2 cycles. For a certain energy threshold, the difference between two energy spectra is reflected in the asymmetry parameter we measure. The energy dependence of the asymmetry can be easily seen. To minimize the statistical error on the precession frequency, the energy threshold is chosen between 1.8-2.0 GeV. For this threshold, the number of events times the square of the asymmetry is maximum.

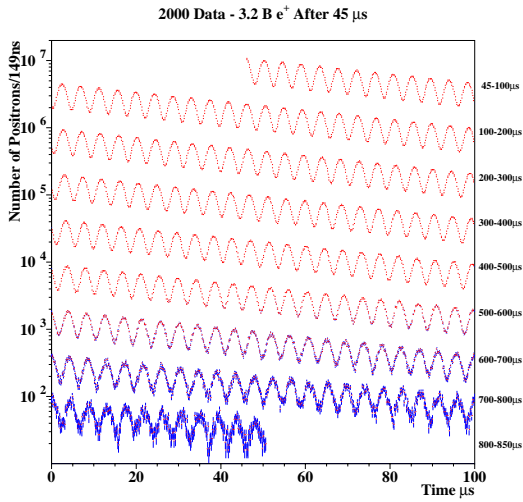


Fig. 1 : g-2 time spectrum. The period of the g-2 is $4.36 \mu\text{s}$ and the dilated lifetime is $64.4 \mu\text{s}$.

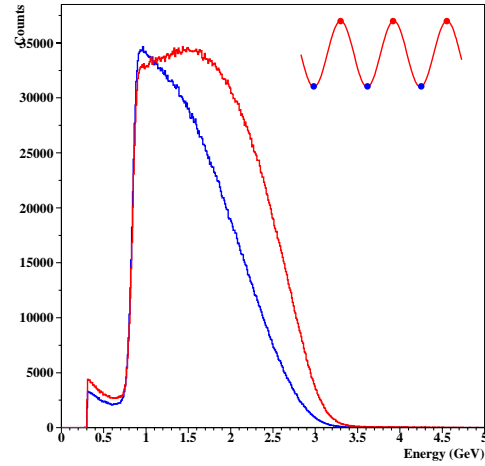


Fig. 2 : A comparison of the positron energy spectrum obtained at the peak and at the trough of g-2.

The BNL g-2 experiment uses a polarized muon beam produced by the Alternating Gradient Synchrotron (AGS), which is the brightest proton source in its energy class in the world. Protons with an energy of 24 GeV hit a nickel target; pions from this reaction are directed into a pion decay channel where they decay into muons. Muons are naturally polarized when a small forward momentum bite is taken.

Our storage ring is a single superconducting C-shape magnet, supplying a 1.45 T uniform field.³ Beam muons are injected into the storage ring through a superconducting inflector magnet, which locally cancels the storage ring field and delivers muons approximately parallel to the central orbit.⁴

The BNL g-2 experiment started first data taking in 1997 using pion injection into the storage ring.⁵ This was similar to what was done in the last CERN experiment.¹ Since the pions fill most of the phase space, there are always a few daughter muons from pion decay which would be captured into stable equilibrium orbits in the storage ring. The disadvantage of pion injection, was the high background level due to the pions themselves. From 1998 on, our experiment used muon injection. In order to put the muons onto their equilibrium orbit, a fast

magnetic kicker was used. The background level was reduced dramatically and the number of events was substantially increased with muon injection compared to pion injection. The kicker is located at 90° with respect to the inflector and consists of three sets of parallel plates each 1.7 m long, carrying 5200 A for a very short time (basewidth 400 ns).⁶

Electrostatic quadrupoles⁷ are used to vertically confine the muons. Four quadrupole assemblies are located in the ring, each pulsed with ± 24 kV and covering 43% of the azimuth in the storage ring.

Inside the ring, the decay positrons are observed for approximately 600 μ s by 24 electromagnetic shower calorimeters⁸ consisting of scintillating fibers embedded in lead. All positrons above a certain threshold are digitized individually with 400 MHz waveform digitizers and the digitized waveforms are stored for the analysis.

3 ω_a Analysis

The g-2 frequency ω_a is determined by fitting the time spectrum of positrons after data selection. There were four independent analyses of the precession frequency from the 2000 data. However, only one of them⁹ is going to be described here.

When statistics are high, the influence of small effects becomes observable in the data. Deviations in the χ^2 and the parameter stability when experimental conditions are varied are the signature of the size of these effects. The 2000 data amount to four times the number of events recorded in 1999. Positron pileup, coherent betatron oscillations (CBO) and muon losses were already observed in 1999 and accounted for in the fitting function.¹⁰ The mismatch between the inflector and storage ring acceptances is one of the main sources of CBO. CBO is also caused by a non-ideal kick to muons when they first enter the ring. Therefore, they are not captured in their equilibrium orbit, but rather oscillate about it. As a result of these oscillations, the beam gets closer and further away from the detectors resulting in a modulation of the counting rate. CBO can be easily seen in the residuals constructed from the difference between the data and the ideal 5-parameter fit (Eq.3 and Fig. 3). The Fourier transform of the residuals is shown in Figure 4.

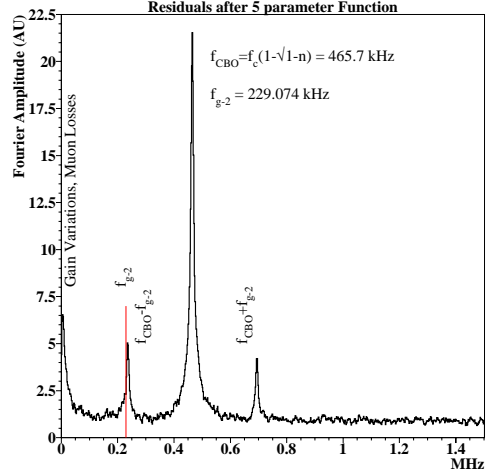
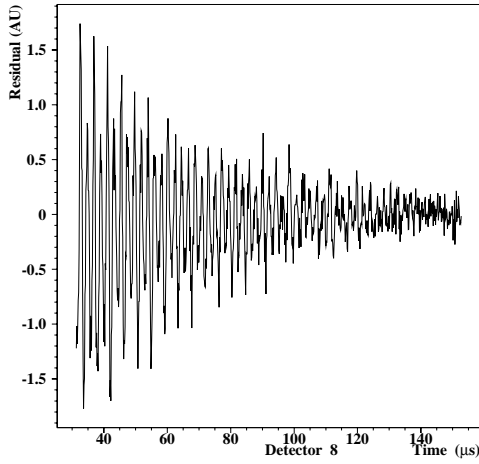


Fig. 3 : Time spectrum of the residuals. **Fig. 4** : Fourier spectrum of the residuals.

Modulations due to CBO are parameterized as:

$$F_{cbo}(t) = 1 + A_{cbo} e^{-t/\tau_{cbo}} \cos[2\pi f_{cbo}t + \phi_{cbo}] \quad (4)$$

where A_{cbo} is the amplitude of the modulation, τ_{cbo} is the coherence time of the damping, and ϕ_{cbo} is the phase. The frequency f_{cbo} is fixed to the frequency determined by the Fourier analysis (465.7 ± 0.1 kHz) of the residuals. With the larger data set from 2000, additionally the g-2 asymmetry (A) and the phase (ϕ) are also seen to be modulated with the CBO. Therefore, the fitting function (Eq. 3) was modified as follows :

$$N(t) = N_0 F_{cbo}(t) e^{-t/\tau_\mu} (1 + A(t) \cos[\omega_a t + \phi(t)]) \quad (5)$$

where

$$A(t) = A (1 + A_A e^{-t/\tau_{cbo}} \cos[\omega_{cbo}t + \phi_A]) \quad (6)$$

and

$$\phi(t) = \phi + A_\phi e^{-t/\tau_{cbo}} \cos[\omega_{cbo}t + \phi_\phi]. \quad (7)$$

The amplitudes A_{cbo} , A_A and A_ϕ are small ($\approx 1\%$, $\approx 0.1\%$ and ≈ 1 mrad, respectively) and are consistent with Monte Carlo simulation.

To avoid beam resonances, the weak-focusing index n was set at 0.137, half way between two neighboring resonances (Figure 5). Running at a higher n value

was not possible because the high voltage on the quads was limited to avoid breakdown. Running at a lower n value leads to storing less beam. Running at $n = 0.137$ made the CBO frequency close to two times the g-2 frequency, which was a difficulty for the analysis, especially for the fit.

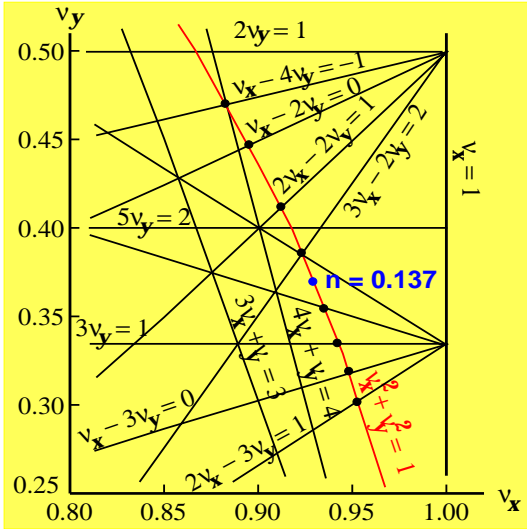


Fig. 5 : Beam tune and n value. The lines represent the resonances.

Pileup, the overlap of positron signals in time, leads to a misidentification of positrons, their arrival time and their energy. Pileup events have half the lifetime of the muons. The size of the effect is larger at early times compared to late times. The way the data was stored permitted us to resolve pileup using the data itself. It was preferred to subtract the pileup events from the data because including the pileup related terms into the

fitting function caused cross-talk between the fit parameters and an increase by a factor of two in the uncertainty of ω_a . Pileup pulses were reconstructed artificially from the data itself in the following way. Every positron pulse above a relatively high threshold is digitized at 400 MHz for 80 ns, which is called a “WFD island”. Positron pulses are fitted with a pulse-finding algorithm to determine energy and time information. This pulse-finding algorithm can resolve only events that are more than 3 ns apart. After the main triggering pulse, there may be a second pulse on the WFD island, which carries the necessary energy and time information for artificial pileup construction. When there is a main triggering pulse, we looked for a secondary pulse on the same WFD island within a time window offset from the trigger. If there is a pulse, the main and the secondary pulses are added properly and the time is assigned from the energy-weighted time of the pair (Figure 6). These constructed pileup events are then subtracted from the data to obtain a pileup-free time spectrum. Figure 7 shows the fit to constructed pileup.

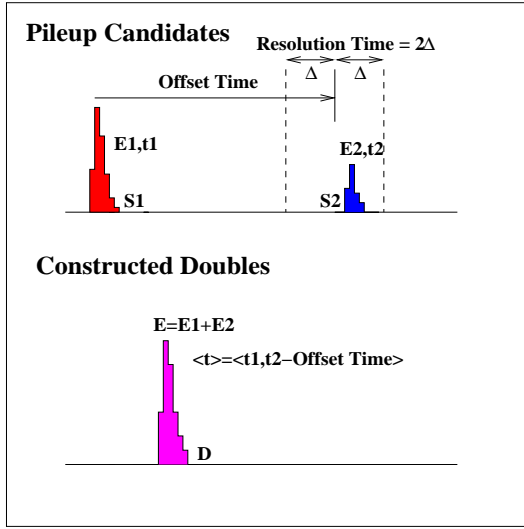


Fig. 6 : Schematic view of the pileup construction.

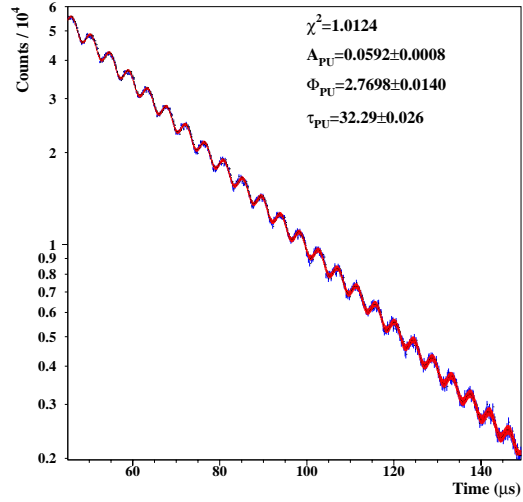


Fig. 7 : Fit to constructed pileup.

One of the tests of checking the pileup subtraction quality is to look at the average energy versus time. The average energy of the detected positrons, for a given g-2 period, with and without the pileup subtraction, is shown in Figure 8. The effect of pileup can be seen clearly in the upper curve. After the pileup subtraction the average energy versus time is flat (lower curve).

The next step in the analysis was to include muon losses. The muon losses were determined two different ways. The pileup subtracted data were fitted at later times ($\approx 300\mu\text{s}$) to an 8-parameter functional form (Ideal+CBO) and extrapolated to earlier times. Only the CBO related parameters were determined at $50\mu\text{s}$ since the lifetime of the CBO is $\approx 110\mu\text{s}$. The ratio of the data to the extrapolated fitting function shows the effect of the lost muons. The second method is to look at three-fold coincidences through consecutive scintillator detectors. Since energy loss for muons is much smaller compared to positrons in the calorimeters, muons can travel between consecutive detectors with little energy loss. The dashed line in Figure 9 is the muon losses determined from these three fold coincidences. The agreement between the two methods is good. The muon loss time spectrum is empirically added to the fitting function with a scale factor, which is a fit parameter.

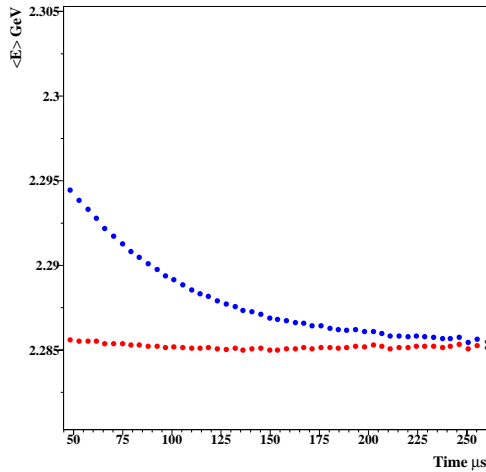


Fig. 8 : Average energy vs time with (lower) and without (upper) the pileup subtraction.

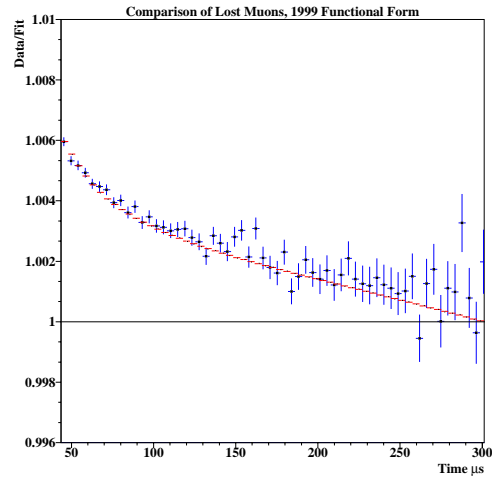


Fig. 9 : Muon losses.

It has been previously mentioned that the n was 0.137. This brought some difficulties to the analysis since $\omega_{cbo} - \omega_a$ was very close to ω_a . The fit had a difficult time to separate these two frequencies. Therefore, we had a considerable systematic effect on ω_a . However, the CBO phase changes from 0 to 2π around the storage ring. For that reason, when the data from individual detectors are added, this effect becomes almost four times smaller. On the other hand when one looks at the precession frequency determined from the individual detectors, the effect is visible. Figure 10 shows the g-2 precession frequency obtained from the individual detectors. The fitting function used here was the ideal five parameter function including modulation of the number of detected events caused by CBO (total 8 parameter). A fit to the data in Fig 10 gives a χ^2/DOF for a fit to a constant, which is unacceptable. When these data are fit to a sine wave (the CBO phase changes 0 to 2π around the ring), the χ^2/DOF becomes acceptable (Fig. 10). The central values on ω_a for both fits are very close.

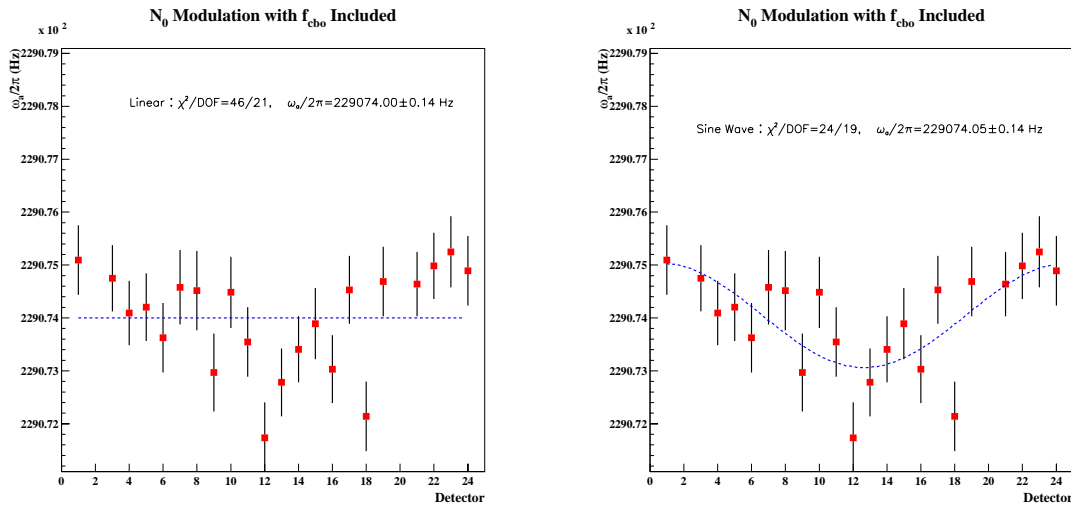


Fig. 10 : Precession frequency vs detectors when the acceptance change due to CBO is included in the fits.

The next step was to make the fitting function more precise by adding the known effects of energy modulation. One of these effects is the modulation of the g-2 asymmetry by CBO. The amplitude of the sine wave is reduced dramatically since most of the effect was removed (Fig. 11). Figure 12 represents the result when both asymmetry and phase modulations are included into the fit.

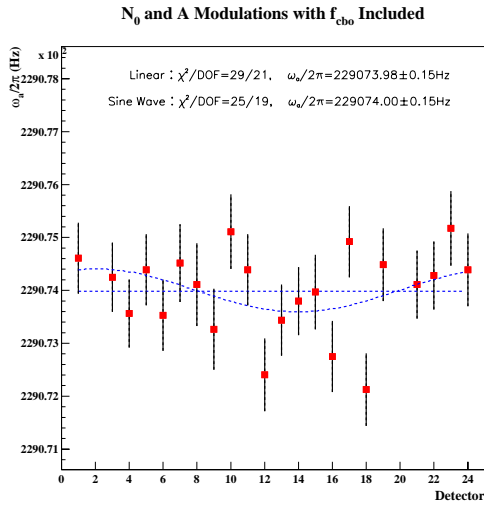


Fig. 11 : Precession frequency vs detectors when asymmetry modulation due to CBO is included in the fit function.

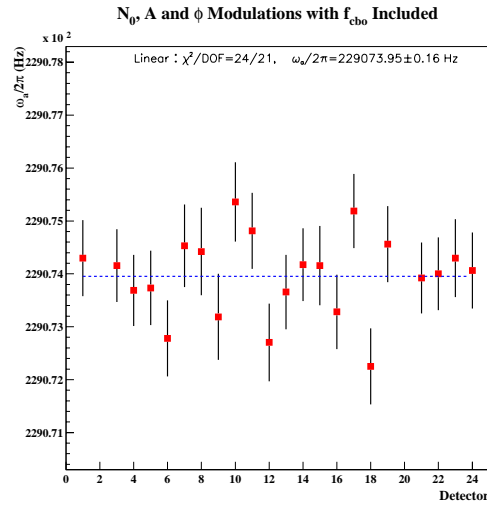


Fig. 12 : Precession frequency vs detectors when both asymmetry and phase modulations are included in the fits.

This study showed that the effect can be removed completely by adding all known effects to the fitting function. However, the center frequency value is not very sensitive to the type of functional form used.

Another method was pursued in the analysis. That was to sample the time spectrum with the CBO period,¹¹ so any CBO related effects can be removed from the data and it can be fit to a five parameter ideal function. The result of this method was consistent with the result of the method described in detail above.

The described analysis determined the precession frequency with 0.7 ppm statistical error. The most significant contributions to the systematic error were CBO (0.21 ppm), pileup (0.13 ppm), gain changes (0.13 ppm), lost muons (0.10 ppm) and fitting procedure (0.06 ppm).

4 ω_p Analysis

The magnetic field B is obtained from NMR measurements of the proton resonance frequency in water, which can be related to the free proton resonance frequency ω_p .¹² The field is continuously measured using about 150 fixed NMR probes distributed around the ring, in the top and bottom walls of the vacuum chamber. In addition to this measurement, the field inside the storage ring where the muons are, is mapped with a trolley device. This device carries 17 NMR probes on it and the measurements were repeated periodically 2-3 times a week.

The trolley moves inside the storage ring and measures the field around the ring without breaking the vacuum. Figure 13 shows a two-dimensional multipole expansion of the field averaged over azimuth from a trolley measurement. The total systematic uncertainty from the field measurements is 0.24 ppm. Figure 14 shows the field map in the storage ring.

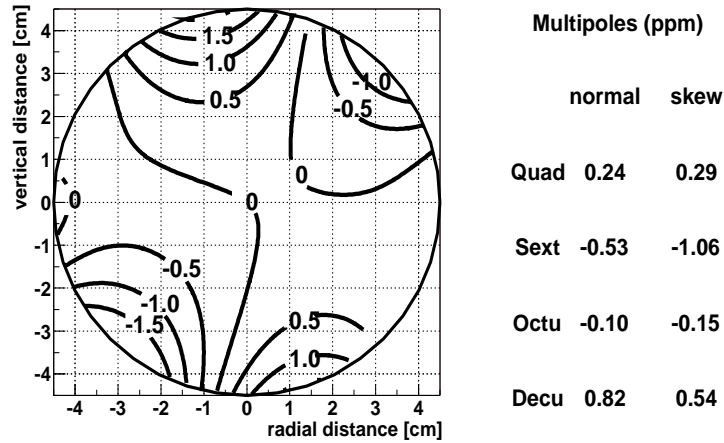


Fig. 13 : Contour plot of multipole expansion.

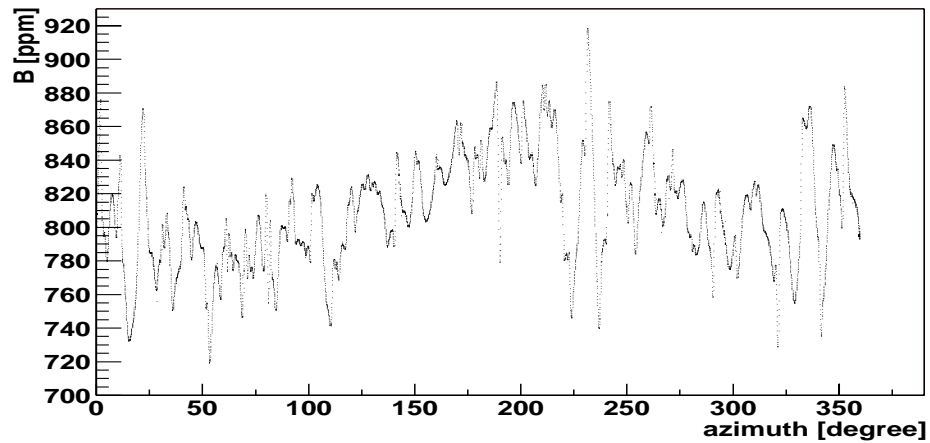


Fig. 14 : Magnetic field map.

5 Result

The anomaly a_μ can be obtained from the result of the independently analyzed frequencies ω_a and ω_p , and is determined to be

$$a_\mu = \frac{\omega_a}{\frac{e}{m\mu} \langle B \rangle} = \frac{\omega_a/\omega_p}{\mu_\mu/\mu_p - \omega_a/\omega_p}. \quad (8)$$

Figure 15 shows the comparison of the last three BNL results with the SM evaluation.

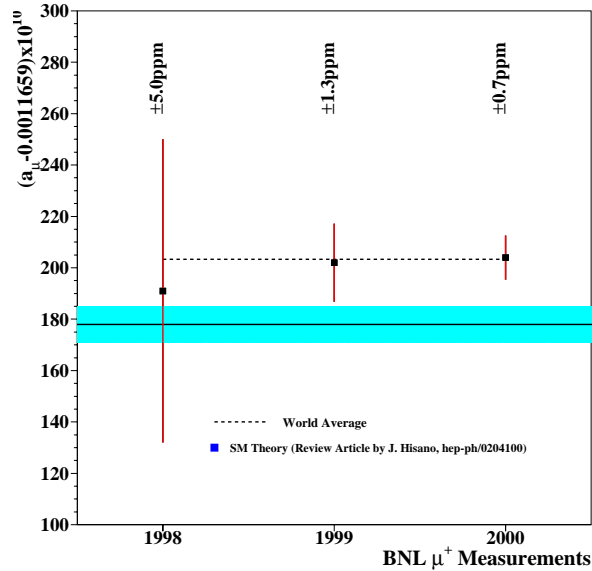


Fig. 15 : Comparison of theory and recent BNL results.

The theoretical value of a_μ in the SM is determined from $a_\mu(\text{SM}) = a_\mu(\text{QED}) + a_\mu(\text{had}) + a_\mu(\text{weak})$. The QED and weak contributions are given by¹³ $a_\mu(\text{QED}) = 11\,658\,470.57(0.29) \times 10^{-10}$ (0.25 ppm) and $a_\mu(\text{weak}) = 15.1(04) \times 10^{-10}$ (0.03 ppm). The leading-order contribution from hadronic vacuum polarization contributes the largest uncertainty to $a_\mu(\text{SM})$. Until recently, $a_\mu(\text{had}, 1) = 692(6) \times 10^{-10}$ (0.6 ppm) was the most reliable value,^{14,15} where data from both hadronic τ -decay and e^+e^- annihilation were used to obtain a single value for $a_\mu(\text{had}, 1)$. Recently, two new evaluations^{16,17} using the new e^+e^- results from Novosibirsk¹⁸ have become available, and Ref.¹⁶ also employs data from hadronic τ -decay. While the two new analyses of e^+e^- data agree quite well, the value of $a_\mu(\text{had}, 1)$ obtained from τ -decay does not agree with the value obtained from e^+e^- data.¹⁶

The higher-order hadronic contributions include¹⁹ $a_\mu(\text{had}, 2) = -10.0(0.6) \times 10^{-10}$ and the contribution from hadronic light-by-light scattering is²⁰ $a_\mu(\text{had}, \text{lbl}) = +8.6(3.2) \times 10^{-10}$. Using the published value of $a_\mu(\text{had}, 1)$ from Ref.¹⁴ the standard model value is $a_\mu(\text{SM}) = 11\,659\,177(7) \times 10^{-10}$ (0.6 ppm).

From the most recent measurements at BNL, the muon anomalous magnetic moment is determined as $a_\mu(\text{exp}) = 11\,659\,204(7)(5) \times 10^{-10}$ (0.7 ppm)²¹ and the difference between $a_\mu(\text{exp})$ and $a_\mu(\text{SM})$ above is about 2.6 times the combined

statistical and theoretical uncertainty. If the new e^+e^- evaluations are used^{16,17} the discrepancy is about 3 standard deviations, and using the τ -analysis alone gives a 1.6 standard deviation discrepancy.

In the 2001 run, the muon g-2 experiment at BNL took data with negative muons with a similar statistical power to the 2000 data. This measurement will provide a test of CPT violation and also an improved value of a_μ .

References

- [1] J. Bailey *et al*, Nucl. Phys. Lett. **B150**, 1(1979) and references therein.
- [2] W. Liu *et al*, Phys. Rev. Lett. **82**, 711(1999); D.E. Groom *et al*, Eur. Phys. J. **C15**, 1(2000).
- [3] G.T. Danby *et al*., Nucl. Instrum. Meth. **A457**, 151(2001).
- [4] A. Yamamoto *et al*., Nucl. Instrum. Meth. **A491**, 23(2002).
- [5] R.M. Carey *et al*, Phys. Rev. Lett. **82**, 1632(1999).
- [6] E. Efstathiadis *et al*, accepted for publication in Nucl. Instrum. Meth.
- [7] Y.K. Semertzidis *et al*, accepted for publication in Nucl. Instrum. Meth. A.
- [8] S.A. Sedykh *et al*, Nucl. Instrum. Meth. **A455**, 346(2000).
- [9] Cenap S. Özben, BNL g-2 internal note, # 423 (2002).
- [10] H.N. Brown *et al*, Phys. Rev. Lett. **86**, 2227(2001).
- [11] This method was originally developed by our collaboration member Yuri Orlov, Cornell University, Ithaca 14853, NY.
- [12] X. Fei, V.W. Hughes, and R. Prigl, Nucl. Instrum. Meth. **A394**, 349(1997); R. Prigl *et al*, Nucl. Instrum. Meth. **A374**, 118(1996).
- [13] A. Czarnecki and W. Marciano, Phys. Rev. **D64**, 012014(2001).
- [14] M. Davier and A. Höcker Phys. Lett. **B435**, 427 (1998).
- [15] The calculations by S. Narison, Phys. Lett. **B513**, 53 (2001) and J.F. de Trocóniz and J.F. Ynduráin, Phys. Rev. **D65**, 093001(2001) used preliminary data from Novosibirsk, and cannot be compared with other analyses.

- [16] M. Davier, S. Eidelman, A. Höcker and Z. Zhang, hep-ph-0208177, Aug., 2002.
- [17] K. Hagiwara, A.D. Martin, Daisuke Nomura and T. Teubner, hep-ph/0209187, Sept. 2002.
- [18] R.R. Akhmetshin, et al., Phys. Lett. **B527**, 161 (2002).
- [19] B. Krause, Phys. Lett. **B390**, 392(1997); R. Alemany, M. Davier and A. Höcker, Eur. Phys. J C2, 123 (1998).
- [20] M. Knecht and A. Nyffeler, Phys. Rev. **D65**, 073034 (2002); M. Knecht, A. Nyffeler, M. Perrottet, E. De Rafael, Phys. Rev. Lett. **88**, 071802 (2002); M. Hayakawa and T. Kinoshita, hep-ph/-112102; J. Bijnens, E. Pallante and J. Prades, Nucl. Phys. **B626**, 410 (2002), I. Blokland, A. Czarnecki and K. Melnikov, Phys. Rev. Lett. **88**, 071803.
- [21] G.W. Bennett *et al*, Phys. Rev. Lett. **89**, 1001804(2002).